Comparative Approach of Doppler Spectra for Fading Channel Modelling by the Filtered White Gaussian Noise Method

Michel Mfeze[1] and Emmanuel Tonye[2]

[1,2]LETS Laboratory, National Advanced School of Engineering, University of Yaounde I, Cameroon
[1]mfeze@yahoo.fr, [2]tonyee@hotmail.com

Abstract– Temporal complexity, bit error rate (BER) testing, and second order statistics like autocorrelation, level crossing rate (LCR) and average fade duration (AFD) play a significant role in fading channel modelling. These parameters describe the channel behaviour, the quality of the fading and the performance of the communication system. The present work focussed on the frequency non selective Rayleigh fading channel and on the filtered white Gaussian noise (FWGN) modelling method. Various Doppler spectra were evaluated through the above mentioned metrics using a Monte Carlo or a semi analytical method. The BER test was performed on two types of LTE (Long Term Evolution) single path channels: the ETU (Extended Typical Urban) channel and the EVA (Extended Vehicular A) channel. The transmitted signal was either M-PSK (M-ary Phase Shift Keying) or M-QAM (M-ary Quadrature Amplitude Modulation) modulated. Matlab was used as simulation tool. The objective being to discriminate and detect the best compromise among all considered Doppler spectra, for an appropriate design of the front-end digital communication system.

Index Terms– Rayleigh Fading, Channel Modelling, Doppler Spectrum, Autocorrelation, Correlogram, BER and LTE

I. INTRODUCTION

CHANNEL modelling allows the demonstration of the channel behaviour from fading statistics through the estimation and computation of its various- order statistics parameters. Those parameters are derived from the design and performance evaluation model of the communication system. Channel models are classified into two main categories: deterministic or analytical channel models and statistical or stochastic models. The deterministic models are derived from received signals empirical measurements, their correlation and distribution. For the statistical models, the channel is time-varying or time-evolving. Assumptions and states are different for each observation. In this case, the assumption of wide sense stationary and uncorrelated scattering (WSSUS) is used to simplify mathematical modelling by stochastic process of the time varying nature of the mobile radio channel in both time and frequency domains.

The additive Gaussian white noise (AGWN) is widely used in communications theory as a beginning for the development and performance evaluation of basic systems. But this model is not adequate for the real channel which is a fading channel. Therefore a more complex and precise model is necessary.

Two groups of methods are mostly encountered in literature for channel modelling and simulation. Jakes' method or Sum-of-Sinusoids methods (including Zheng & Xiao, Pop & Beaulieu, modified Hoeher etc) where the complex envelop of the channel is a sum of homogenous components or oscillators, each characterized by its amplitude, frequency and phase. Rayleigh fading is achieved with a high number of oscillators and is a solid mathematical model for the real channel where there is generally no line of sight between the transmitter and the receiver. The FWGN methods (including Smith (based on Clarke model), Young, etc) which are explored in this paper simulate the channel properties through signal processing techniques, with no need to consider the underlying propagation mechanism. The white Gaussian noise is filtered using a Doppler spectrum based filter. The most important first and second order fading statistics parameters can be then captured.

The present work considers a number of Doppler spectra from literature to filter the white Gaussian noise. Then the frequency non-selective channel behaviour is studied through signal quality, and second order statistics like average fade duration (AFD), level crossing rate (LCR), or autocorrelation function (ACF). These parameters give a more detailed behaviour of the channel [1]. Finally, digital modulation techniques can improve communication systems by increasing capacity, speed and transmission quality. Those which have been explored for the fading channel performance evaluation through bit error rate are the M-PSK and M-QAM as they are used in the multi-carriers OFDM (Orthogonal Frequency Division Multiplexing) used by 3G and 4G technologies [2]. In OFDM, modulated data are transmitted simultaneously on many sub-carriers, allowing high data rates. Also, the BER of an OFDM signal is similar to the BER of the underlying modulation technique in a Gaussian channel, and is much better for a Rayleigh channel than a wideband CDMA (Code Division Multiple Access) signal using the same modulation technique. Therefore, simulating the performance of the channel on the above modulation techniques is a good step prior to OFDM case study. The powerful processing capabilities of Matlab software package were used for the simulations.

For a LTE channel of 5MHz bandwidth, the sample period is 0.1302µs for a sampling frequency f of 7.68MHz. That frequency is double for a 10MHz bandwidth. The LTE norm defines three channel models. The EPA (Extended Pedestrian A model) channel with a maximum Doppler frequency fdm of 5Hz, the EVA channel with fdm=70Hz and the ETU channel with fdm=300Hz. A LTE frame lasts 10ms with 20 slots of 0.5ms each. If each slot contains 7 OFDM symbols, the duration of the fading sequence would be 140 symbols.

II. MATHEMATICAL MODELLING OF A FADING MULTIPATH CHANNEL

The received signal at the fading channel output is the sum of the different paths and is given by:

$$x(t) = Re\{[\sum_n \alpha_n(t)e^{-j2\pi f_c \tau_n(t)}S(t - \tau_n(t))]e^{j2\pi f_c t}\} + \eta(t) \quad (1)$$

with α_n, the attenuation factor of the signal received through the nth path, $\tau_n(t)$ is its delay which is time varying, $\eta(t)$ is the additive white Gaussian noise, f_c is the carrier frequency and $S(t)$ is the complex envelop of the transmitted signal. The baseband signal will be affected by attenuations $\alpha_n(t)$, delays $\tau_n(t)$ and phase shifts $-j2\pi f_c \tau_n(t)$ which are all time varying.

The equivalent low pass signal is:

$$r_l(t) = \sum_n \alpha_n(t)e^{-j2\pi f_c \tau_n(t)}S(t - \tau_n(t)) \quad (2)$$

Equation (1) defines the baseband transfer function as follows:

$$h(t, \tau) = \sum_n \alpha_n(t)e^{-j2\pi f_c \tau_n(t)}\delta(t - \tau_n(t)) \quad (3)$$

$h(t, \tau)$ is the channel impulse response at time t to a pulse applied at instant $t-\tau$. In $h(t, \tau)$ formula, τ and t represent the time axis and the delay axis respectively. δ is the Dirac function. By minimizing the noise component, the received signal can be written as a convolution of the transmitted signal s(t) and the channel impulse response $h(t, \tau)$.

$$r(t) = s(t) * h(t, \tau) \quad (4)$$

If $\delta=1$, the received signal is:

$$r(t) = \sum_n \alpha_n(t)e^{-j2\pi f_c \tau_n(t)} \quad (5)$$

The gains $\alpha_n(t)$ vary slowly and there should be a great variation in the channel to affect the signal amplitude whereas phase shifts present higher variation rate for high speeds and carrier frequencies. For a high number of paths, the central limit theorem applies and the envelop $h(t, \tau)$ can be modelled as a complex random Gaussian process which is Rayleigh distributed. The channel can be described in frequency domain and Doppler frquency domain using four functions.

A. The Impulse Response h(t, τ, φ)

The channel effect lying on time and delays only can be studied in the time domain using this function. The output and input of the channel are linked by the following convolution

$$r(t) = \int_{-\infty}^{+\infty} s(\tau, \varphi)h(t - \tau, \varphi)d\tau = \int_{-\infty}^{+\infty} s(t - \tau, \varphi)h(t, \tau, \varphi)d\tau \quad (6)$$

Equation (6) can be re-written as a sum [3]:

$$r(t) = \Delta\tau \sum_m s(t - m\Delta\tau, \varphi).h(t, m\Delta\tau, \varphi) \quad (7)$$

With this new formulation, the frequency selective channel in the time domain can be represented as a tapped delay line (TDL) using path gains and delays as shown in Fig. 1.
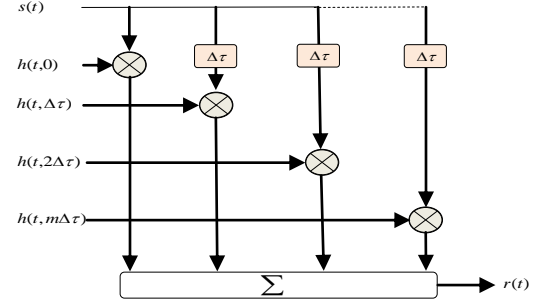

Fig. 1. Tapped Delay Line TDL representation of the multipath channel

described in frequency domain and Doppler frequency domain using four functions.

B. The Delay-Doppler Diffusion Function D(τ,v,φ)

This is a delay-Doppler shift channel description. The function $D(\tau,v,\varphi)$ and the impulse response of the channel are linked by a Fourier transform as follows:

$$D(\tau, v, \varphi) = \int_{-\infty}^{+\infty} h(t, \tau, \varphi).e^{-j2\pi f_c \tau}dt \quad (8)$$

The channel output is then:

$$r(\tau, \varphi) = \int_{-\infty}^{+\infty}\int_{-\infty}^{+\infty} s(t - \tau, \varphi)D(\tau, v, \varphi).e^{-j2\pi v\tau}dv\, dt \quad (9)$$

C. The Time-Frequency Description: the Transfer Function H(f, t, φ)

The transfer function is a link between the temporal output of the channel filter and the input signal and determines the frequency selectivity of the propagation channel.

$$H(f, t, \varphi) = \int_{-\infty}^{+\infty} h(t, \tau, \varphi).e^{-j2\pi f_c \tau}d\tau = \int_{-\infty}^{+\infty} G(f, v, \varphi).e^{-j2\pi v\tau}dv \quad (10)$$

described in frequency domain and Doppler frequency domain using four functions.

D. The Output Doppler Spread G(f, v, φ)

This function describes the channel in the $f - v$ domain. The Doppler shift is also given by this function, which is a shadow of the impulse response $h(t, \tau, \varphi)$ in the frequency-Doppler shift domain. The function is also a link between the output spectrum of the channel $R(f, \varphi)$ and the input spectrum $S(f, \varphi)$ as follows:

$$R(f, \varphi) = \int_{-\infty}^{+\infty} s(f - v, \varphi)G(f, v, \varphi)dv \quad (11)$$

The above functions are commonly designed by Bello functions [4] and are linked to each other by either a Fourier Transform (FT) or an Inverse Fourier Transform (IFT) as shown in Fig. 2.
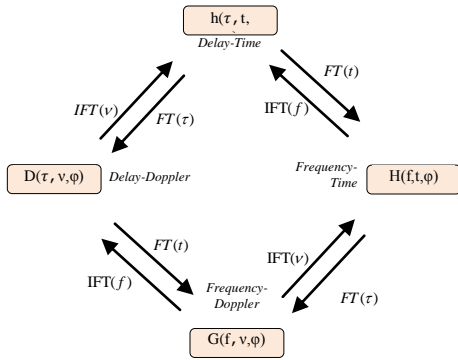

Fig. 2. The four channel functions

III. FREQUENCY DISTORTION: THE DOPPLER EFFECT

This is generated in a mobile transmission by a moving transmitter or receiver and leads to an apparent shift of the received signal frequency resulting in temporal variations of phases and amplitudes. The frequency shift on the nth path is given by:

$$f_{dn} = f_c - f_{in} = \frac{V}{c} f_c cos\theta_n = f_{Dmax} cos\theta_n \qquad (12)$$

V is the mobile speed in m/s. f_{in} is the instantaneous frequency in Hz of the signal received through the nth path, c is the light speed and θ_n is the angle between the mobile and the received wave through the nth path. The output of the channel is:

$$r(t) = cos(2\pi f_c t) \sum_n \alpha_n cos(2\pi f_{dn} t + \varphi_n)$$
$$-sin(2\pi f_c t) \sum_n \alpha_n sin(2\pi f_{dn} t + \varphi_n) \qquad (13)$$

IV. STATISTICAL CHARACTERIZATION OF THE MULTIPATH CHANNEL

A. First-Order Statistics

1) The gain Probability Density Function (PDF)

For the complex Gaussian gain $\bar{h}(t)$ it is given by [5].

$$p(|\bar{h}|) = \frac{r}{2\pi\sigma_h^2} e^{-\frac{|\bar{h}|^2}{\sigma_h^2}} \qquad (14)$$

2) The variance σ_h^2

The expression of the variance of the signal is:

$$\sigma_h^2 = \frac{1}{2} E\left(|\bar{h}(t)|^2\right) = \frac{1}{2} E(\bar{h}_r(t)^2) + \frac{1}{2} E(\bar{h}_i(t)^2) \qquad (15)$$

3) The Instantaneous Power

This parameter determines the signal to noise ratio at the receiver.

$$z = r^2 = |\bar{h}|^2 \qquad (16)$$

E. Second-Order Statistics

1) The Power Delay Profile $P(\tau)$

This is the average channel output power as a function of delays.

$$P(\tau) = \frac{\sigma_h^2}{\tau_{rms}} e^{-\frac{\tau}{\tau_{rms}}} \qquad (17)$$

τ^2_{rms} is the delays variance.

2) The Doppler Spectrum

For a mobile with speed V in a multipath fading environment, each Doppler frequency is given by equation (12). By deriving by the incidence angle, we get:

$$\frac{dv}{d\theta_n} = \frac{|\bar{V}|}{c} f_c sin\theta_n = f_{Dmax}\sqrt{1 - cos^2\theta_n} = f_{Dmax}\sqrt{1 - \left(\frac{v}{f_{Dmax}}\right)^2} \qquad (18)$$

For a high number of paths, one can estimate the received power in the direction $d\theta_n$ as the product of the power density $P(\theta_n)$ and the incidence angle $d\theta_n$. Thus, the received power S_H can be related to the Doppler shift f_{dn} to get the Doppler power spectrum $S_H(f_{dn})$:

$$S_H(v) = \frac{P(\theta_n) + P(-\theta_n)}{f_{Dmax}\cdot\sqrt{1 - \left(\frac{v}{f_{Dmax}}\right)^2}} \qquad (19)$$

For an isotropic spread, the total power received from each direction is

$$P(\theta_n) = \frac{\sigma_h^2}{2\pi} \qquad (20)$$

The Doppler spectrum can be written as follows and is commonly named Jakes spectrum.

$$S_H(v) = \frac{\sigma_H^2}{\pi.f_{Dmax}} \frac{1}{\sqrt{1 - \left(\frac{v}{f_{Dmax}}\right)^2}} \qquad (21)$$

Other forms of the Doppler spectrum can be found in the literature and will be described later in this paper [6].

3) The Autocorrelation Function

According to the Wiener–Khintchine theorem, the autocorrelation function is linked to the power spectrum density by a Fourier transform. Therefore, for a random process, the inverse Fourier transform of the power spectrum density is the autocorrelation function. This traduces the correlation between the value of the signal at a given instant and the value of the same signal after a duration τ [7].

$$r_H(\tau) = \int_{-\infty}^{+\infty} S_H(v).e^{j2\pi v\tau} d\tau = \frac{\sigma_H^2}{2\pi} \int_{-\infty}^{+\infty} e^{j2\pi f_{Dmax}.cos\theta_n.\tau} d\theta_n$$
$$= \sigma_H^2.J_0(2\pi f_{Dmax}\tau) = \sigma_H^2.J_0(\frac{2\pi x}{\lambda}) \qquad (22)$$

It can be seen that the autocorrelation depends on the time delay τ and the spatial shift x. The k-order autocorrelation coefficient r_k is given by:

$$r_k = \frac{\sum_{t=k+1}^{n}(g_t - \bar{g}_1)(g_{t-k} - \bar{g}_2)}{\sqrt{\sum_{t=k+1}^{n}(g_t - \bar{g}_1)^2 \sum_{t=k+1}^{n}(g_{t-k} - \bar{g}_2)^2}} \tag{23}$$

with $\bar{g}_1 = \frac{1}{n-k}\sum_{t=k+1}^{n} g_t$ et $\bar{g}_2 = \frac{1}{n-k}\sum_{t=k+1}^{n} g_{t-k}$

The most important r_k is r_1.

4) The Level Crossing Rate

The level crossing rate is a metric of the fading speed and quantify how many times the signal crosses a given threshold ρ in the positive direction. The following formulation is derived from the classical Doppler spectrum.

$$LCR = \sqrt{2\pi} f_{dm} \rho e^{-\rho^2} \tag{24}$$

ρ is the threshold normalized by the root mean square (RMS) of the signal and f_{dm} is the maximum Doppler spectrum.

5) The Average Fade Duration

The average fade duration is the average time the signal is lower than or equal to a given threshold ρ. It is also the average time between two successive level crossing in both directions (negative and positive). The formulation below results from the classical Doppler spectrum.

$$AFD = \frac{1}{\sqrt{2\pi}} \frac{(e^{\rho^2} - 1)}{\rho f_{dm}} = \frac{1 - e^{\rho^2}}{LCR} \tag{25}$$

F. Types of Doppler Spectra

1) Jakes Classical Doppler Spectrum

The Jakes Doppler spectrum is given by [6], [8]:

$$S(f) = \begin{cases} \frac{3}{2\pi f_{dm}} \frac{1}{\sqrt{1 - \left(\frac{f}{f_{dm}}\right)^2}} & |f| \leq f_{dm} \\ 0 & |f| > f_{dm} \end{cases} \tag{26}$$

2) Flat Doppler Spectrum

$$S(f) = \frac{1}{2 f_{dm}}, \quad f_{dm} \neq 0 \tag{7}$$

3) Asymetric Jakes Doppler Spectrum

$$S(f) = \begin{cases} \frac{A}{\pi f_{dm}} \frac{1}{\sqrt{1 - \left(\frac{f}{f_{dm}}\right)^2}}, & -f_{dm} \leq f_{min} \leq f \leq f_{max} \leq f_{dm} \\ 0 & \end{cases} \tag{28}$$

with $A = \frac{\pi}{\left[\sin^{-1}\left(\frac{f_{max}}{f_{dm}}\right) - \sin^{-1}\left(\frac{f_{min}}{f_{dm}}\right)\right]}$

4) Bell Doppler Spectrum

$$S(f) = \begin{cases} a_0 + a_2 \cdot \left(\frac{f}{f_{dm}}\right)^2 + a_4 \cdot \left(\frac{f}{f_{dm}}\right)^4 & |f| \leq f_{dm} \\ 0 & |f| > f_{dm} \end{cases} \tag{29}$$

Where a_0, a_2, and a_4 are real and are the polynomial coefficients of the spectrum.

5) Gaussian Doppler Spectrum

$$S(f) = \begin{cases} \frac{1}{\sqrt{2\pi\sigma^2}} e^{-\frac{f^2}{2\sigma^2}} & |f| \leq f_{dm} \\ 0 & |f| > f_{dm} \end{cases} \tag{30}$$

Where $\sigma = \sigma_g f_{dm}$ with σ_g the standard deviation of the Gaussian classical function.

6) Bi-Gaussian Doppler Spectrum

$$S(f) = \begin{cases} g_1 \frac{1}{\sqrt{2\pi\sigma_1^2}} e^{-\frac{(f-f_{c1})^2}{2\sigma_1^2}} + g_2 \frac{1}{\sqrt{2\pi\sigma_2^2}} e^{-\frac{(f-f_{c2})^2}{2\sigma_2^2}} & |f| \leq f_{dm} \\ 0 & |f| > f_{dm} \end{cases} \tag{31}$$

g_1 and g_2 are the power gains of the Gaussian components with values following a linear scale. f_{c1} and f_{c2} represent the central frequencies of the Gaussian components normalized by the maximum Doppler frequency. Values are therefore within interval [-1,1]. Finally σ_1, σ_2 are real positive and are the standard deviation of the Gaussian function normalized by the maximum Doppler frequency.

f) The Laplacian Doppler Spectrum

$$S(f) = \begin{cases} \frac{e^{-\frac{\sqrt{2}}{\sigma}\left|acos\left(\frac{f}{f_{dm}}\right)-\varphi\right|} + e^{-\frac{\sqrt{2}}{\sigma}\left|acos\left(\frac{f}{f_{dm}}\right)+\varphi\right|}}{\sqrt{1 + 10^{-9} - \left(\frac{f}{f_{dm}}\right)^2}} & |f| \leq f_{dm} \\ 0 & |f| > f_{dm} \end{cases} \tag{32}$$

7) The SUI (Stanford University Interim) Doppler Spectrum

$$S(f) = \begin{cases} 1 - 1.72\left(\frac{f}{f_{dm}}\right)^2 + 0.785\left(\frac{f}{f_{dm}}\right)^4 & |f| \leq f_{dm} \\ 0 & |f| > f_{dm} \end{cases} \tag{33}$$

8) The 3GPP-Rice Doppler Spectrum

$$S(f) = \begin{cases} \frac{0.41}{2\pi f_{dm}} \frac{1}{\sqrt{1 + 10^{-9} - \left(\frac{f}{f_{dm}}\right)^2}} + 0.91\delta(f - 0.7 f_{dm}) & |f| \leq f_{dm} \\ 0 & |f| > f_{dm} \end{cases} \tag{34}$$

V. THE FILTERED WHITE GAUSSIAN NOISE METHOD

Let $H(f)$ be the frequency response of a filter and $x(t)$ a signal with power spectral density $p_x(f)$ being filtered. The power spectral density $p_y(f)$ of the output signal $y(t)$ is given by:

$$p_y(f) = p_x(f)|H(f)|^2 \tag{35}$$

In order to generate In- phase and quadrature components of the channel complex coefficients, each having a Doppler spectrum $p_y(f) = S(f)$, one needs to filter white Gaussian noise with power spectral density $N_0/2$ through a filter $H(f)$ with frequency response

$$H(f) = \sqrt{\frac{2}{N_0} S(f)} \qquad (36)$$

The above filter can be implemented either by Inverse Discrete Fourier Transform (IFDT) or by a regressive filter [5].

A. The Smith's Model

Smith [9] used in-phase I and quadrature Q components concept to simulate Clarke and Gans fading model. This is a translation of equation (3) as shown in Fig. 3.
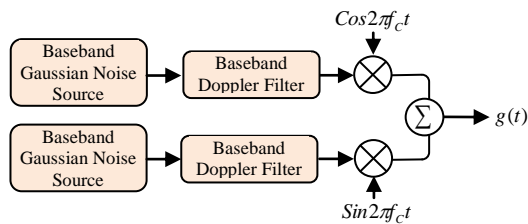
Fig. 3. Clarke and Gans model

Two Gaussian noise sources g_1 and g_2 are used to generate I and Q. Each component is a sum of two real and orthogonal random Gaussian independent variables, a and b. The resulting variable g=a+jb is therefore Gaussian complex. The Jakes Doppler spectrum is then used as a filter. The IFDT is used at the end of the model for frequency domain signal shaping to get time domain precise waves forms [10]. Each Smith noise source is a random Gaussian complex number generator of length Nrv and produces a baseband spectral line with complex weights in the positive frequency band. The spectral line is bounded either side by the maximum Doppler frequency $[-f_{dm} +f_{dm}]$ with equally distributed components along the line. The negative components are the conjugates of the Gaussian complex values for positive frequencies. In order to get correlated signals, the random variables of the spectral line are then multiplied by a discrete frequency representation of $\sqrt{S_E(f)}$ with same length as the noise source. Each filter output is then passed through an Inverse Fast Fourier Transform (IFFT) module and finally the channel output is computed as the sum of the two IFFT modules output.

Smith solved the problem of infinity approach at the limit of bandwidth by truncating $S_E(f)$ then increasing the slope before that limit. The scheme on Fig. 4. shows the Smith's simulation model which is a frequency domain representation of the above model, much easier to implement.

B. Young and Beaulieu Model

David J. Young and Norman C Beaulieu proposed a model [11] also based on IDFT which is a kind of modified Smith's model. According to the authors, this model uses half of the IDFT and only 2/3 of spatial complexity compared to Smith's model. Two independent identically distributed (i.i.d) random
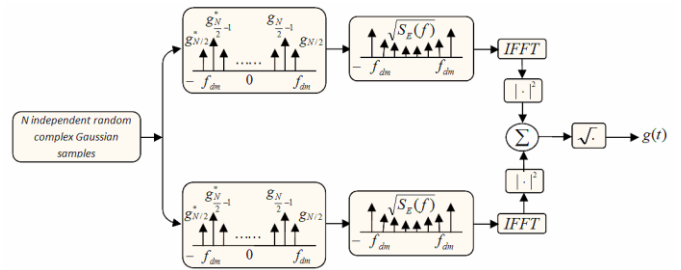

Fig. 4. Smith's fading simulator

Gaussian processes of N components are generated and filtered by two identical low-pass Doppler filter of frequency response $\{F[k]\}$ in order to get correlated signals. The in-phase and quadrature components are added and the result is passed through an IFFT module which gives the channel output signal [12].

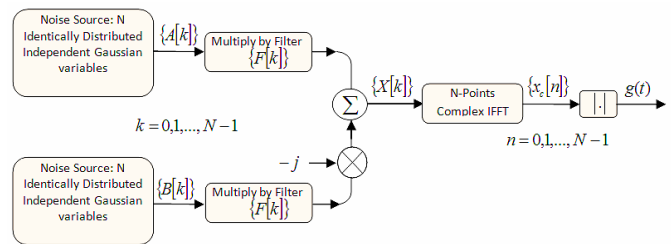Fig. 5. shows the Young's fading simulator [5]

Fig. 5. Young's Fading simulator

The length of the Rayleigh fading sequence generated by this simulator depends on the length of the noise sources which must be high enough to get a reasonable fading sequence length.

The Young's Doppler filter is given below:

$$F_m(k) = \begin{cases} 0, & k = 0 \\ \sqrt{\dfrac{1}{2\sqrt{1-\left(\frac{k}{Nf_m}\right)^2}}} & k = 1,2,\dots,k_m-1 \\ \sqrt{\dfrac{k_m}{2}\left[\dfrac{\pi}{2} - arctan\left(\dfrac{k_m-1}{\sqrt{2k_m-1}}\right)\right]} & k = k_m \\ 0, & k = k_m+1,\dots,N-k_m \\ \sqrt{\dfrac{k_m}{2}\left[\dfrac{\pi}{2} - arctan\left(\dfrac{k_m-1}{\sqrt{2k_m-1}}\right)\right]} & k = N-k_m \\ \sqrt{\dfrac{1}{2\sqrt{1-\left(\frac{N-k}{Nf_m}\right)^2}}} & k = N-k_m+1,\dots,N-1 \end{cases} \qquad (37)$$

where $f_m = \dfrac{f_{Dmax}}{f_s}$ and $k_m = \lfloor Nf_m \rfloor$

Let's emphasize that both Smith and Young' simulators generate a single path fading. For LTE channels with 7 or 9 paths, the algorithms have to be run 7 or 9 times.

VI. METHODOLOGY

Smith proposed a model based on Jakes Doppler spectrum for Gaussian white noise filtering. In this paper, we applied different other Doppler spectra listed previously for comparison means on a non frequency selective fading
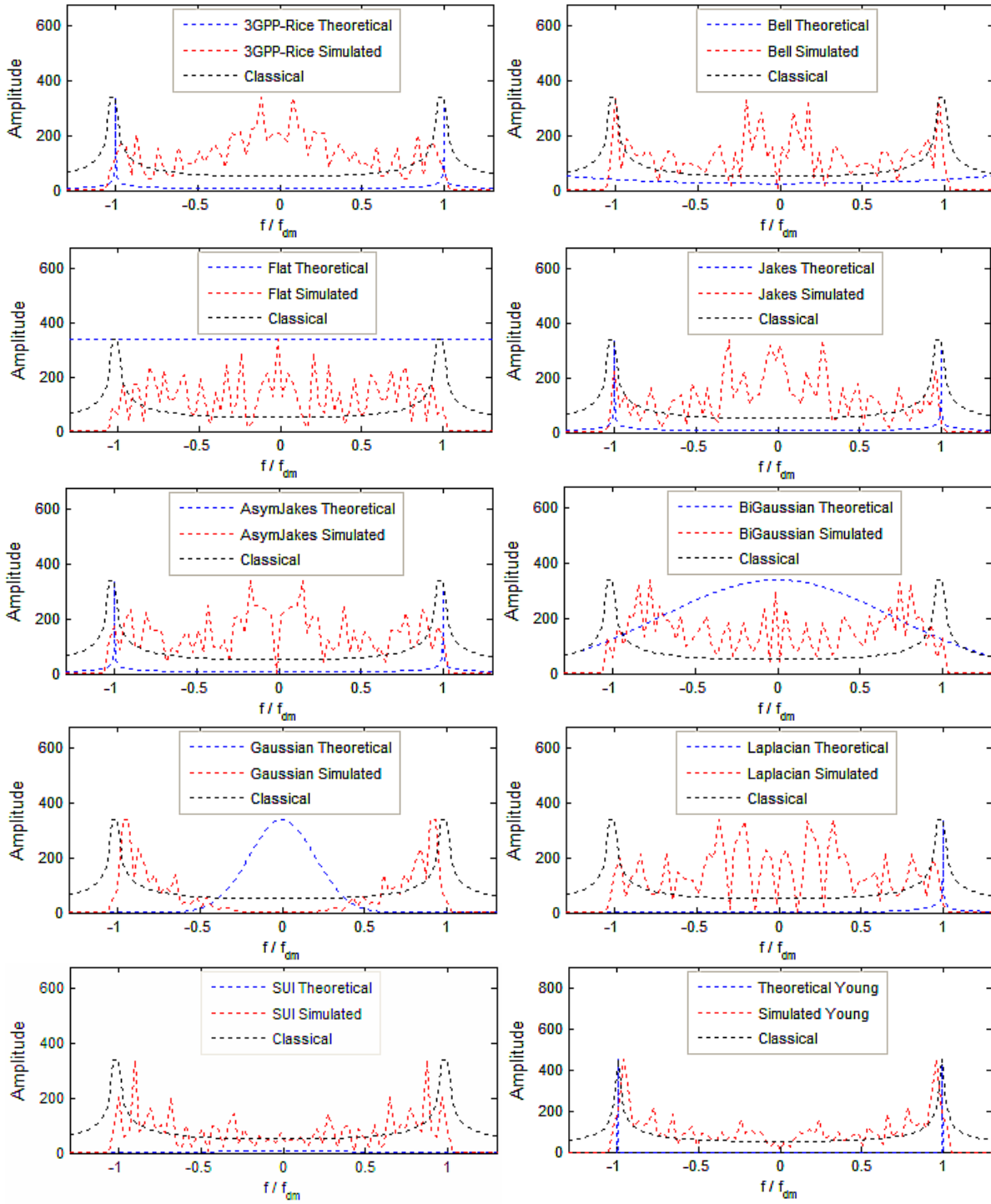
Fig. 6. Theoretical and simulated Doppler spectra for f_{dm}= 50Hz

channel. The temporal complexity was evaluated by computing the processing time of the algorithm for each Doppler spectrum, as a function of gain vector or fading sequence length. This was done using the Matlab *timeit* function. The quality of the signal was also investigated through second order statistics like the LCR, the AFD and the autocorrelation. The randomness of the process affecting the results for each run for LCR and AFD computations, this was overcome by using a Monte Carlo (MC) method through thousands of iterations of the algorithm being executed and then considering values of highest occurrence probability. Correlation coefficients were computed and correlograms were plotted using the following simulation parameters. Nrv=64; V=30km/h; fc=1.8GHz; fs=15 KHz (to reduce

computational load). This gives fdm=50Hz. The observed threshold for LCR was arbitrary set to r0=0.6 or r0=-4.4dB. The speed of the mobile was then doubled (V=60km/h) and the LCR and AFD were re-evaluated.

A last attempt to discriminate Doppler spectra was done by computing the bit error rate which is a very important metric in communications. This was used for performance evaluation of the Rayleigh channel on BPSK, QPSK, 8-PSK, 16-QAM and 64-QAM signals as they are the modulation techniques used by 2G, 3G and OFDM-LTE (4G) wireless technologies [13], [14].

A signal with carrier frequency 1.8GHz is to be passed through a LTE single path channel with bandwidth 5MHz for a sampling frequency of 7.68MHz. For the present case study, the single path was considered in EVA and ETU channels with maximum Doppler frequencies of 70Hz and 300Hz respectively. The generated signal was M-PSK and M-QAM modulated then rectangular pulse shaped. Then it was filtered by the Rayleigh fading channel modelled by the FWGN model using various Doppler spectra. After, white Gaussian noise was added and the signal was injected into the receiver for filtering by an ideal integrator and demodulation. The BER was finally computed using a semi analytical method through Matlab *semianalytic* function. That method was preferred to the MC method which would have a prohibitive computational load. The simulated BER curve was finally compared to the theoretical BER curve.

VII. RESULTS AND DISCUSSION

Fig. 6. shows a plot of the different Doppler spectra against theoretical curve and classical Doppler spectrum curve derived from analytical expression. Young's simulated spectrum appears to be the closest to the theoretical classical spectrum followed by Gaussian and SUI.

The Rayleigh fading sequence generated by Smith and Young' methods are shown in Fig. 7. and Fig. 8. They all happen to be zero mean stationary time series.

A. Temporal Complexity Analysis

Various fading sequence lengths or path gain-vector lengths Ns were simulated and the processing time of both Smith t_s (using various Doppler spectra) and Young t_y were computed. Fig. 9.a shows the obtained curves and Fig. 9.b presents values of processing time for Ns=1625602 samples. For low values of Ns (Ns≤2x10^5), the processing time for the different spectra used on Smith's algorithm are slightly different. The curves have no constant position relative to each other. This is due to the randomness of Gaussian noise sources used by the method. But for greater values of Ns (Ns→∞), the Smith's curves are likely convergent with the same logarithmic progression. The Young's curve presents the same progression but is negatively shifted from the Smith's curves.

Young's algorithm is obviously less time consuming than Smith's algorithm, no matter the Doppler spectrum. But it can be observed that all Doppler spectra applied to Smith's model have similar temporal complexity and even identical for Ns infinite. It was noticed the ratio $\frac{t_y}{t_s}$ can be approximated by a

linear combination of the fading sequence length Ns (Fig. 9) and verifies:

$$\frac{t_y}{t_s} \approx \frac{-8}{10^8} * N_s + 0.7 \quad \text{for fs= 7.68x10}^6, \text{ fdm=300Hz, Ns} \geq 4.5\text{x}10^5 \qquad (38)$$
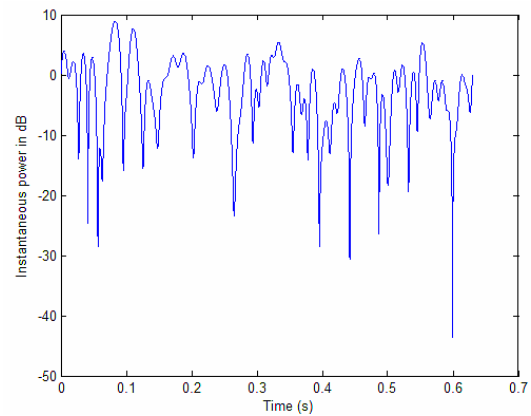

Fig. 7. Rayleigh fading generated by Smith's simulator for fdm= 50Hz
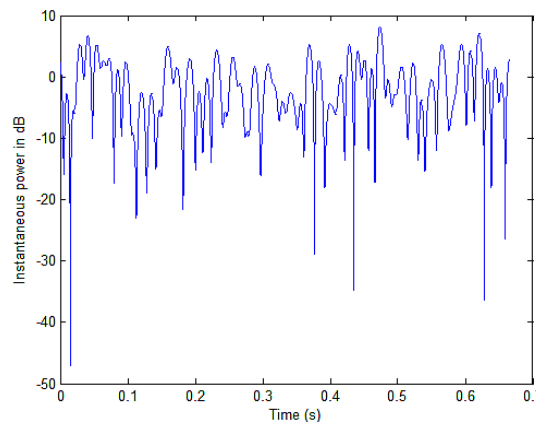

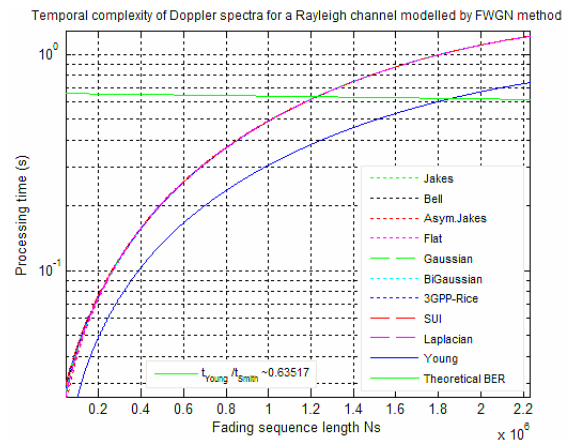Fig. 8. Rayleigh fading generated by Young's simulator for fdm= 50Hz
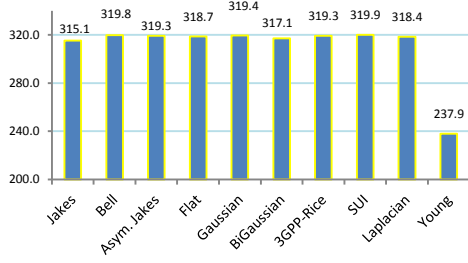

Fig. 9. Temporal complexity: Processing time curves

Fig. 10. Temporal complexity: Sample values for Ns=1625602 in milliseconds

In conclusion, Young's model has less temporal complexity than Smith's model whatever the Doppler spectrum used and is a better modeling and simulation scheme for the Rayleigh fading channel.

B. Autocorrelation and Correlograms

In order to confirm the above assumption, it might be useful to draw autocorrelation curves or correlograms. The autocorrelation is an index which is often used to measure the persistence of the signal in a fading channel. Fig. 11 shows correlograms of path gains for a fading channel modelled by Smith's method using different Doppler spectra, and also, by Young's method. They all are in good agreement with the theoretical result. Adjacent observations of the channel are also highly correlated for all Doppler spectra and mostly for very short delays ($\tau \to 0$). Moreover, all correlograms periodically converge back towards zero. This confirms the randomness of the underlying time series representing the fading. Positive autocorrelation also denotes persistence of data or of the states of frequency non selective Rayleigh channel. The rapid decrease of the correlation coefficient from 1 to 0 for increasing delays denotes the shortness of the signal and confirms the WSS assumption.

For delays less than 10ms, the Gaussian Doppler spectrum gives the shortest signal, followed by the Young's spectrum whereas the longest one would be the Laplacian. Young's model gives a better correlation and its curve is the closest to the theoretical curve for delays less than 10ms. Correlograms also show different peaks even though the periodicity is almost the same and thus demonstrate different behaviors of the channel due to the Doppler filter used in the model. Fig. 12 shows the first order correlation coefficients obtained from the distributions in Fig. 13. They all converge towards unity for higher values of the sampling frequency fs.

C. Normalized Level Crossing Rate and Average Fade Duration

Two values of mobile speed were considered. V1=30km/h for fdm=50Hz (Fig. 14 and Fig. 15), and V2=60km/h for fdm=100Hz (Fig. 16 and Fig. 17). The LCR and AFD curves are in agreement with the theoretical curves for all spectra. The maximum values of LCR are found around -3dB. The lower the mobile speed, the lower the LCR and the higher the AFD. The best agreement with theoretical curves is given by

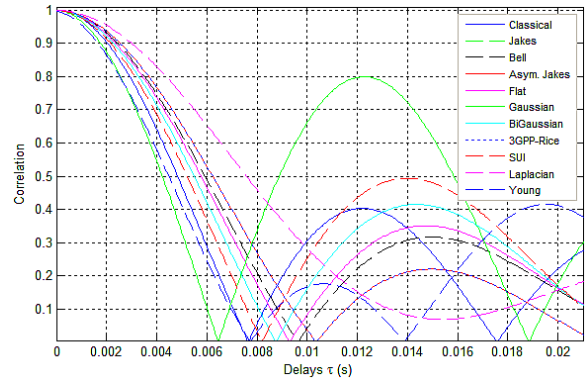the Young's model followed by the Smith's model using SUI Doppler spectrum.
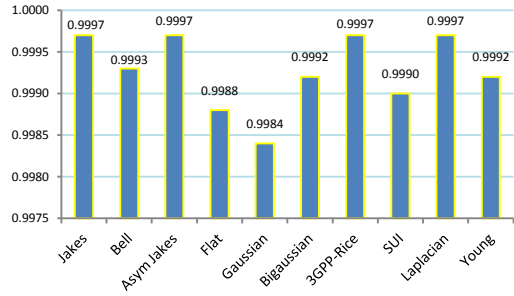

Fig. 11. Correlograms for fdm= 50Hz and fs=15 KHz

Fig. 12. First-order correlation coefficients
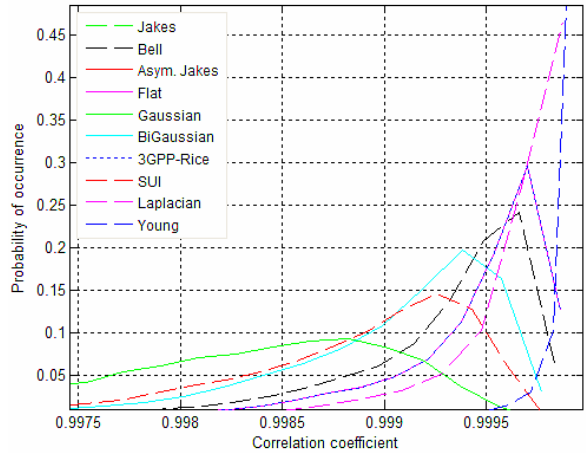

Fig. 13. Distribution of first order correlation coefficients for fdm=50Hz and fs=15 KHz simulated by a Monte Carlo Method.

In addition, all curves keep the same position relative to each other. The Gaussian spectrum produces the highest LCR for the lowest AFD and the Laplacian filter gives the lowest LCR for the highest AFD. Jakes, asymmetric Jakes and 3GPP-Rice spectra present similar performances. In that case, further investigation on other performance indices like the bit error rate needs to be performed.
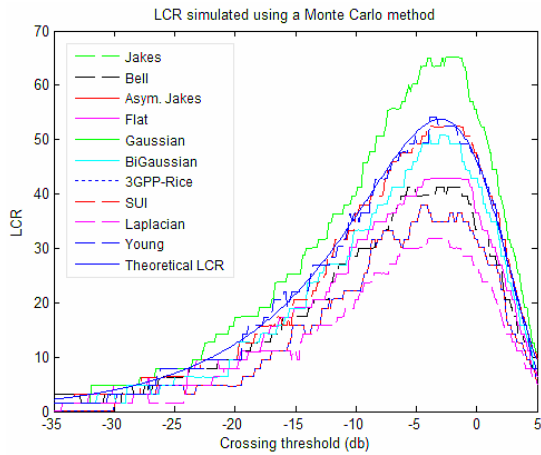
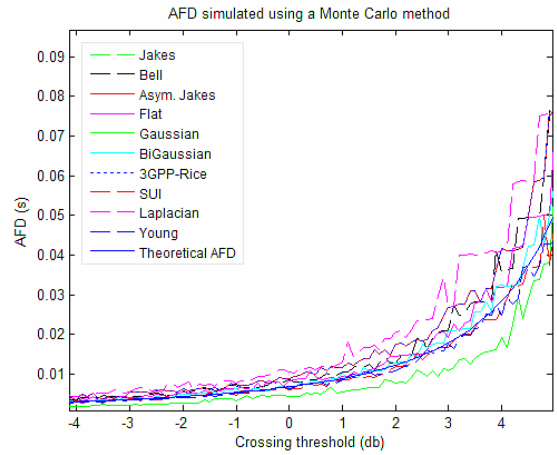Fig. 14. Simulated against Theoretical LCR for V=30km/h

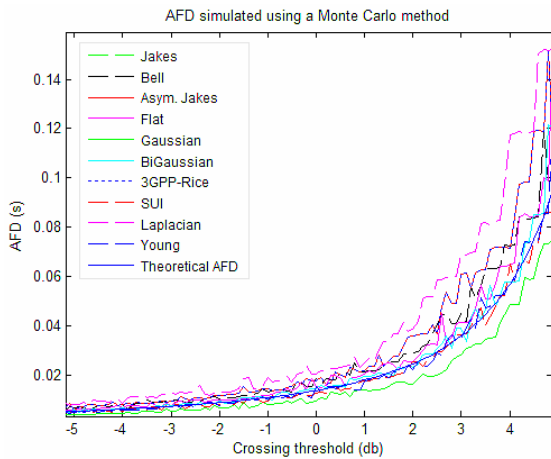Fig. 15. Simulated against Theoretical AFD for V=30km/h
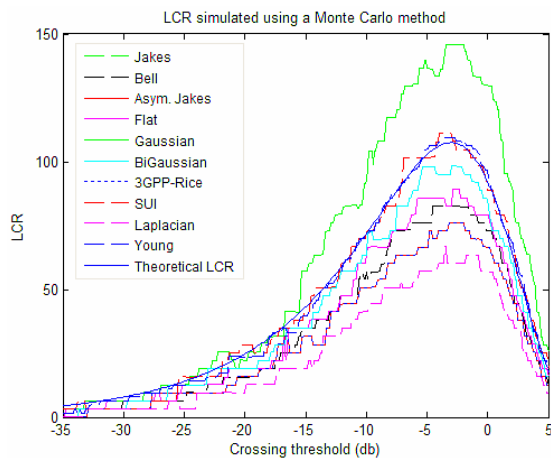

Fig.16. Simulated against Theoretical LCR for V=60km/h

Fig.17. Simulated against Theoretical AFD for V=60km/h

D. Bit Error Rate

Performance evaluation of Rayleigh fading channel is done through the BER computation using the following modulation techniques: BPSK (2-PSK), QPSK (4-PSK), 8-PSK, 16-QAM and 64-QAM. A LTE channel is considered with bandwidth 5MHz, and maximum Doppler frequencies of 70Hz and 300Hz corresponding to EVA and ETU environments respectively. The sampling frequency is 7.68MHz. The bit error rate is a key performance indicator of the data link through a Rayleigh fading channel and the system performance is inversely proportional to the BER. In the case of 64-QAM modulation and for both EVA and ETU channels, the BER is below the theoretical BER curve for Eb/No values less than or equal to 15dB. The simulated BER curve is above the theoretical curve for Eb/No values greater than 15dB. In the case of 16-QAM, the crossing is found at a much lower value of Eb/No (8dB) for both environments (Fig. 18, Fig. 19, Fig. 20 and Fig. 21).

In the case of PSK modulation (Fig. 22 to Fig. 27), the simulated BER curve is always above the theoretical curve and for all Doppler spectra. In addition, confirmation is made in both PSK and QAM cases that higher modulation order schemes which allows higher data rates are also more sensitive to noise as they produce a higher BER curve. Furthermore, lower order modulation techniques are more robust and produce BER curves closer to the theoretical curve, but are limited in term of data rates. Finally the figures shows the beam of BER curves is more convergent in ETU environment (high speed), than in EVA environment (lower speeds).
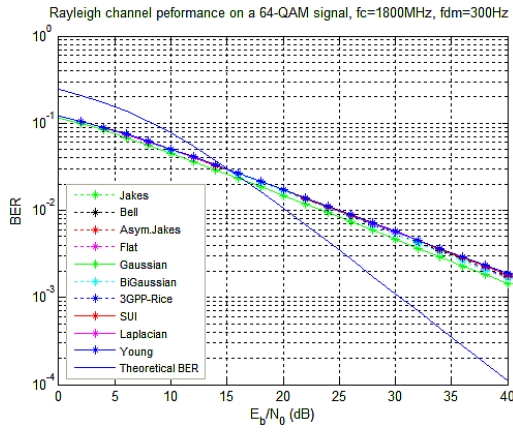
Fig. 18. Rayleigh channel performance on a 64-QAM signal for V=180km/h
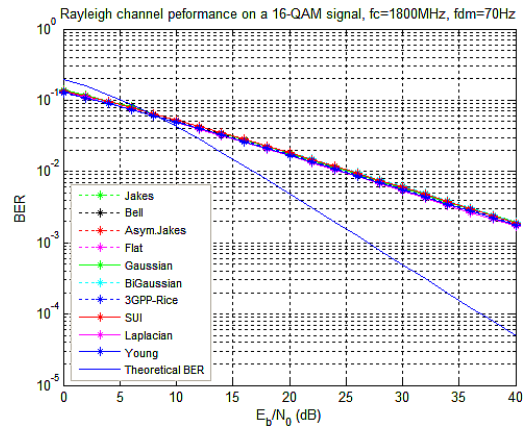

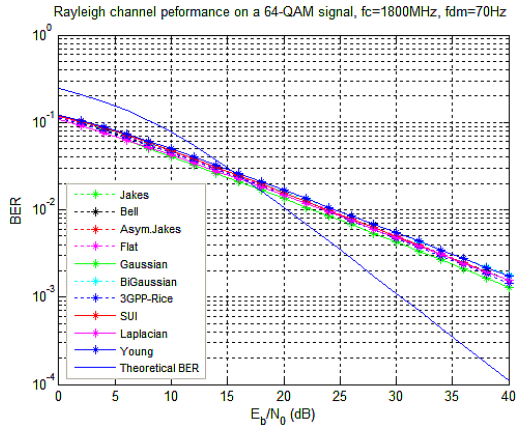Fig. 21. Rayleigh channel performance on a 16-QAM signal for V=42km/h

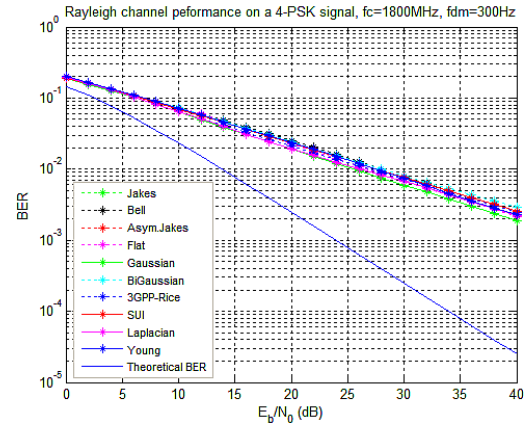Fig. 19. Rayleigh channel performance on a 64-QAM signal for V=42km/h

Fig. 22. Rayleigh channel performance on a QPSK signal for V=180km/h
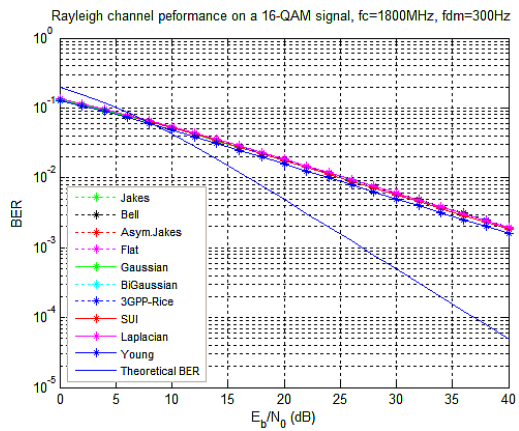

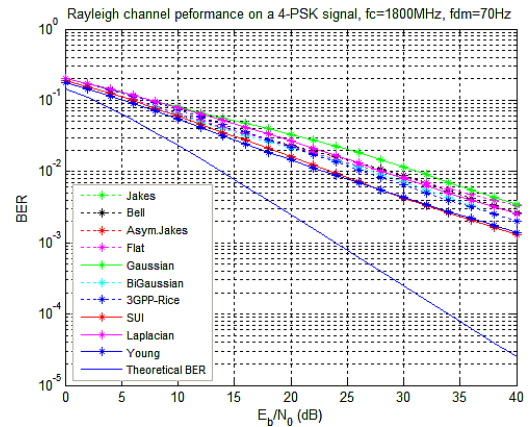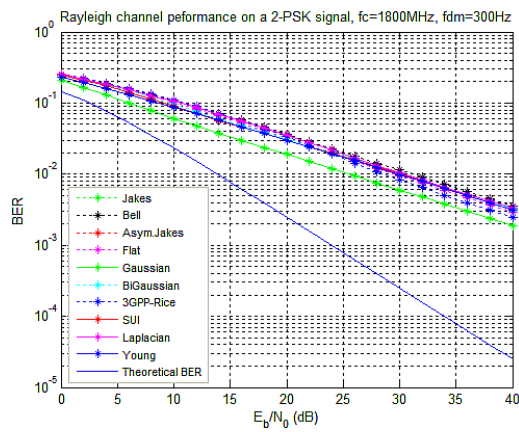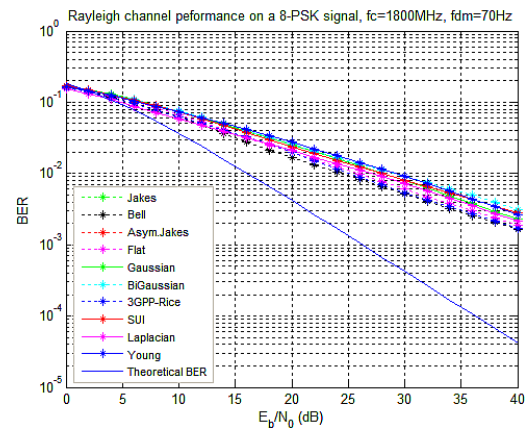Fig. 20. Rayleigh channel performance on a 16-QAM signal for V=180km/h

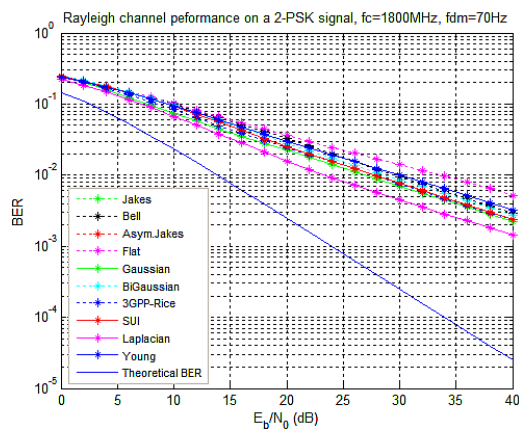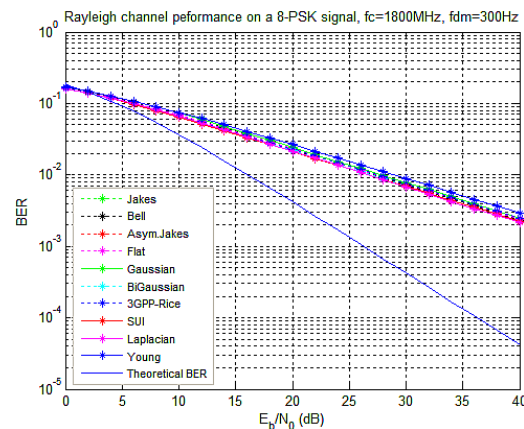Fig. 23. Rayleigh channel performance on a QPSK signal for V=42km/h

Fig. 24. Rayleigh channel performance on a BPSK signal for V=180km/h

Fig. 27. Rayleigh channel performance on a 8-PSK signal for V=42km/h

Fig. 25. Rayleigh channel performance on a BPSK signal for V=42km/h

VIII.   CONCLUSION

In this paper, various Doppler spectra were evaluated for modelling the frequency non-selective Rayleigh fading channel by the filtered white Gaussian noise method. To achieve this, the Smith's model using all considered Doppler spectra, and the Young's model were simulated with key parameters like temporal complexity, second order statistics (autocorrelation, level crossing rate, average fade duration) being examined and curves plotted against the expected theoretical curves. The effect of maximum Doppler frequency variation was also investigated. The randomness of the process affects the results for the FWGN modelling method. This was overcome by using a Monte Carlo simulation scheme through thousands of iterations of the algorithm being executed and then considering values of highest occurrence probability. This allowed us to provide a deterministic solution to an initially stochastic problem. Above all this, a comparative evaluation of the BER computed by a semi analytic method for LTE-ETU and LTE-EVA channels was performed and finally Young's model appeared to be a better channel modelling and simulation compromise followed by the Smith's model using SUI Doppler spectrum.

REFERENCES

[1]   Anjana Jain, Prakash D. Vyavahare, Leeladhar Arya, "Estimation of Fading Statistics of Nakagami Channel with Weibull Distributed Tolerable Outage Time," Shri G. S. Institute of Technology and Science, Indore, India, Wireless Engineering and Technology, 2012, 3, 77-82.

[2]   Ravi Kant Gupta, Anuj Jain, Prashant Singodiya, "Bit error rate simulation using 16-QAM technique in Matlab," International Journal of Multidisciplinary Research and Development, Volume :2, Issue :5, 59-64 May 2015

[3]   J.D. Parsons, The Mobile radio propagation channel, Second Edition, John Wiley & Sons Ltd, 2000.

[4]   Khawar Siddique Khokhar, "Design and development of mobile channel simulators using digital signal processing techniques, "Durham theses, Durham University. 2006, PP44-46.   [Online].   Available: http://etheses.dur.ac.uk/2948/.

Fig. 26. Rayleigh channel performance on a 8-PSK signal for V=180km/h

[5] Ali Arsal, "A study on wireless channel models: Simulation of fading, shadowing and further applications, " M. Eng. thesis, Izmir Institute of Technology. August 2008.

[6] Yong Soo Cho, Jaekwon Kim, Won Young Yang, Chung G. Kang, MIMO-OFDM wireless communications with MATLAB, Ed John Wiley & Sons (Asia) Pte Ltd, 2010.

[7] Ahmed Saadani, Méthodes de Simulations Rapides du Lien Radio pour les Systèmes 3G, Thèse de Doctorat, Ecole Nationale Supérieure de Paris, Décembre 2003.

[8] Cyril-Daniel Iskander, " A MATLAB -based Object-Oriented Approach to Multipath Fading Channel Simulation," Hi-Tek Multisystems, Québec, QC, Canada, G1H 3V9.

[9] John I. Smith, " A Computer Generated Multipath Fading Simulation for Mobile Radio," IEEE Transactions on Vehicular Technology, vol VT-24, No. 3, August 1975.

[10] Theodore S. Rappaport, Wireless Communications: Principles and Practice (2nd Edition), Ed Prentice Hall, 2002.

[11] David J. Young and Norman C. Beaulieu, " The generation of correlated Rayleigh random variates by inverse discrete Fourier transform," IEEE transactions on Communications, vol. 48, pp. 1114-1127, July 2000.

[12] Abdellah Berdai, " Egalisation aveugle et turbo égalisation dans les canaux sélectifs en fréquence invariants et variant dans le temps, " Mémoire de maîtrise en génie électrique. Université Laval. Québec, 2006.

[13] Houman Zarrinkoub, Understanding LTE with Matlab. From mathematical modelling to simulation and prototyping, Ed John Wiley & Sons Ltd, 2014.

[14] Yannick Bouguen, Éric Hardouin, François-Xavier Wolff, *LTE et les réseaux 4G,* Sous la direction de Guy Pujolle, Editions Groupe Eyrolles, 2012 Chapitre 1.